# Fundamental Properties of Radiation From a Leaky Mode Excited on a Planar Transmission Line

William L. Langston, *Student Member, IEEE*, Jeffery T. Williams, David R. Jackson, *Fellow, IEEE*, and Francisco Mesa, *Member, IEEE*

***Abstract*—By using a specific normalization, it is shown that the $\mathrm{TM}_0$ *radiation field* from a leaky mode that is excited by a source on *any* printed-circuit structure can be represented in a unified manner. The general properties of the normalized leaky-mode radiation field are examined in detail for a variety of phase and attenuation constants, as well as distances from the source, and for different types of source excitations. The normalized leaky-mode radiation field is compared to similarly normalized geometrical-optics and far-field radiation expressions to provide further insight into the nature of the radiation fields in the near- and far-field regions. The results provide a general view of leaky-mode radiation properties independent of the type of planar transmission line or background structure.**

***Index Terms*—Crosstalk, leaky-mode excitation, leaky waves, microstrip, printed circuits, radiation, stripline.**

## I. Introduction

THE existence of dominant (quasi-TEM) leaky modes on printed-circuit transmission lines has been a subject of considerable interest. These modes are usually undesirable since they can result in increased attenuation, signal distortion, crosstalk with nearby components, and other spurious effects. Dominant leaky modes have been found on a number of planar transmission-line structures including multilayer stripline, microstrip line, covered microstrip, coplanar strips, and coplanar waveguide [1]–[10]. As opposed to higher order leaky modes [11], dominant leaky modes have a quasi-TEM current distribution, which makes these modes particularly problematic in integrated-circuit transmission-line structures.

Most studies involving leaky modes have focused on a specific structure, showing results for the wavenumber of the leaky mode or (more recently) for the current or field of the leaky mode when excited by a source [12]–[14]. Hence, the conclusions from these studies are tied to specific structures (although many of the conclusions are applicable to a variety of structures). The purpose of this paper is to draw *general conclusions* about the leaky-mode fields that are excited by a source *independent of the structure*. Results are shown for both "physical" and "nonphysical" in the "spectral-gap" region.

Manuscript received April 17, 2003. This work was supported in part by the Texas Advanced Research and Technology Program. The work of F. Mesa was supported by Spanish McyT and FEDER under Project TIC2001-3163.

W. L. Langston, J. T. Williams, and D. R. Jackson are with the Department of Electrical and Computer Engineering, University of Houston, Houston, TX 77204-4005 USA.

F. Mesa is with the Department of Applied Physics 1, University of Seville, Seville 41012, Spain.

Digital Object Identifier 10.1109/TMTT.2003.819777

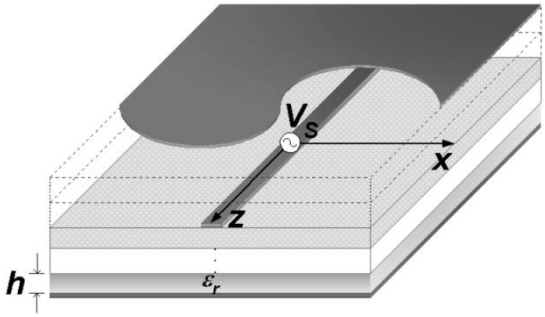


Fig. 1. Geometry of a general planar transmission line with a finite gap source $V_s$.

It is shown here that, by using a specific normalization, the fields radiated by a leaky mode that is excited by a source on *any printed-circuit structure* can be represented in the same unified manner. The results apply to any type of infinite or semi-infinite printed transmission line with a single conducting strip (such as mutilayer stripline, microstrip, covered microstrip, etc.) that is excited by a localized source, provided the leakage is only into the $\mathrm{TM}_0$ mode of the background structure. Results for other types of structures can also be obtained using superposition (coplanar strips) or following the same method of analysis assuming a magnetic current (slotline) instead of an electric current. For open structures, the space-wave leakage can also be formulated in a normalized manner using a similar procedure.

Three general types of leaky-mode currents are considered, which cover all practical source excitations of interest. These currents correspond to an infinite line with an even bi-directional leaky-mode current, an infinite line with an odd bi-directional leaky-mode current, and a semi-infinite line with a unidirectional leaky-mode current. The characteristics of the radiation fields from these leaky-mode currents are studied in detail as a function of the leaky-mode phase constant (leakage angle) and attenuation (leakage) constant. The characteristics studied include the amplitude distribution of the radiation field, power flow in the radiation field, and "effective point of radiation" for a leaky mode, which has not been previously defined. In addition, results are presented for a geometrical optics (GO) approximation to the radiation field to explore the accuracy and limitations of this approximation. A far-field approximation to the radiation field is also presented and compared with the exact results.

A general planar transmission line is considered for the analysis provided in this paper. A diagram of a planar transmis-

sion-line structure with a small, but finite gap source ($V_S = 1\,\mathrm{V}$) is shown in Fig. 1. (This type of source excites an even-mode current on the transmission line. Other types of sources will be discussed later.) Although this figure shows a covered microstrip configuration, the analysis is general and applies to any printed-circuit structure. The conducting strip is assumed to be infinite in the $\pm z$-directions and all of the conductors are assumed to be perfect. For simplicity, the strip width $W$ is assumed to be small so that the transverse component of the current can be neglected.

## II. Leaky-Mode Radiation Field

### A. Analysis

Assuming that the $\mathrm{TM}_0$ mode of the background structure is the only mode above cutoff, the fields radiated by the strip current into this mode (i.e., the radiation field) can be formulated by calculating the fields radiated into this mode by a $z$-directed infinitesimal electric dipole, and then integrating over the strip current [12]

$$E_y(x,y,z) = A(y)\int_{-\infty}^{+\infty} I(z')H_1^{(2)}\left(k_{\mathrm{TM}_0}\rho'\right)\cos(\phi')dz' \quad (1)$$

where

$$\rho' = \sqrt{(x)^2 + (z-z')^2} \quad (2)$$

$$\cos(\phi') = \frac{z-z'}{\rho'} \quad (3)$$

and $A(y)$ is a function that gives the $y$-variation of the fields due to the dipole. This function is different for each type of transmission line and can be calculated using standard spectral-domain techniques.

To obtain a general normalized form for the radiation field, the strip current $I(z')$ is assumed to be a leaky-mode current that is bi-directionally excited by a source, such as the gap voltage source shown in Fig. 1. Such a source excites an even-mode current (with respect to $z'$). (A similar analysis applies for the case of an odd-mode current excitation or the case of a unidirectional current excited on a semi-infinite line $z' > 0$.) The even leaky-mode current is represented as

$$I(z') = A_{\mathrm{LM}}e^{-jk_z|z'|} \quad (4)$$

where $A_{\mathrm{LM}}$ is the complex excitation coefficient for the leaky mode and $k_z = \beta_z - j\alpha_z$ is the propagation wavenumber of the leaky mode. All the distances in (1) are normalized by the $\mathrm{TM}_0$-mode wavelength $\lambda_{\mathrm{TM}_0} = 2\pi/k_{\mathrm{TM}_0}$ (i.e. $\bar{x} = x/\lambda_{\mathrm{TM}_0}$, $\bar{z} = z/\lambda_{\mathrm{TM}_0}$, $\bar{\rho} = \rho/\lambda_{\mathrm{TM}_0}$) and the phase and attenuation constants are normalized by the $\mathrm{TM}_0$-mode wavenumber $k_{\mathrm{TM}_0}$ (i.e., $\bar{\beta}_z = \beta_z/k_{\mathrm{TM}_0}$, $\bar{\alpha}_z = \alpha_z/k_{\mathrm{TM}_0}$). After some simple calculations, the vertical electric field radiated by the strip current is written as

$$E_y(\bar{x},\bar{y},\bar{z}) = A_N\int_{-\infty}^{+\infty} e^{-j(\bar{\beta}_z - j\bar{\alpha}_z)2\pi|\bar{z}'|}H_1^{(2)}(2\pi\bar{\rho}')\cos(\phi')d\bar{z}' \quad (5)$$

where

$$A_N = A(y)A_{\mathrm{LM}}\lambda_{\mathrm{TM}_0} \quad (6)$$

is a constant (for a fixed value of $y$) that only depends on the parameters of the specific background structure. Note that, to within a multiplicative factor, the radiation field (5) at a given normalized observation position $(\bar{x}, \bar{z})$ is solely a function of the normalized constants $\bar{\alpha}_z$ and $\bar{\beta}_z$ for any printed-circuit structure that is excited by a bi-directional even-mode source. For a source that excites a bi-directional odd-mode current (such as a vertical probe or via), the integrand in (5) is modified by multiplication with $\mathrm{sgn}(z')$. For a semi-infinite line that is excited by a source at the end, the integral in (5) is modified by simply replacing the lower limit of integration with zero.

In this paper, $\bar{\beta}_z$ will often be specified indirectly by choosing a value for the approximate leakage angle $\phi_0$ in accordance with the relation

$$\phi_0 = \cos^{-1}\left(\bar{\beta}_z\right) \quad (7)$$

which provides accurate predictions of the leakage angle for small $\bar{\alpha}_z$. (The exact leakage angle is in the direction of the phase vector with components ($\beta_x$ and $\beta_z$).) The results in this paper are for the normalized radiation field, as represented by the integral in (5), or for quantities such as the Poynting vector that come from the normalized field. The unnormalized (absolute) field for any specific structure may be obtained by scaling the normalized field results by the normalization constant $A_N$.

### B. Physical Leaky-Mode Results

The results in this section are for a physical leaky mode. A physical leaky mode is a mode that is a fast wave with respect to $k_{\mathrm{TM}_0}$ ($\bar{\beta}_z < 1$). Results will be presented for a variety of values for $\bar{\beta}_z$ and $\bar{\alpha}_z$, which are treated as independent parameters to make the results as general as possible. Of course, for an actual structure, the two values are related. An example showing such a relationship for a specific structure, and how the general methodology developed here may be applied to the structure, will be given in Section VIII.

In Fig. 2, the magnitude of the normalized leaky-mode radiation field is plotted for $\phi_0 = 50°$ and $\bar{\alpha}_z = 0.001, 0.01, 0.1$, respectively. For $\bar{\alpha}_z = 0.001$, the radiation field inside a triangular leakage region or "lit region" is seen to be very strong. This radiation picture closely resembles that for a GO field, in which "rays" emanate from the line at the leakage angle to illuminate the leakage region, and the field is very small (essentially zero) in the "shadow region." In the approximate GO model, the field is uniform along the lines of leakage within the lit region. One interesting feature observed in Fig. 2(a) is the oscillatory nature of the field within the lit region as the observation point moves

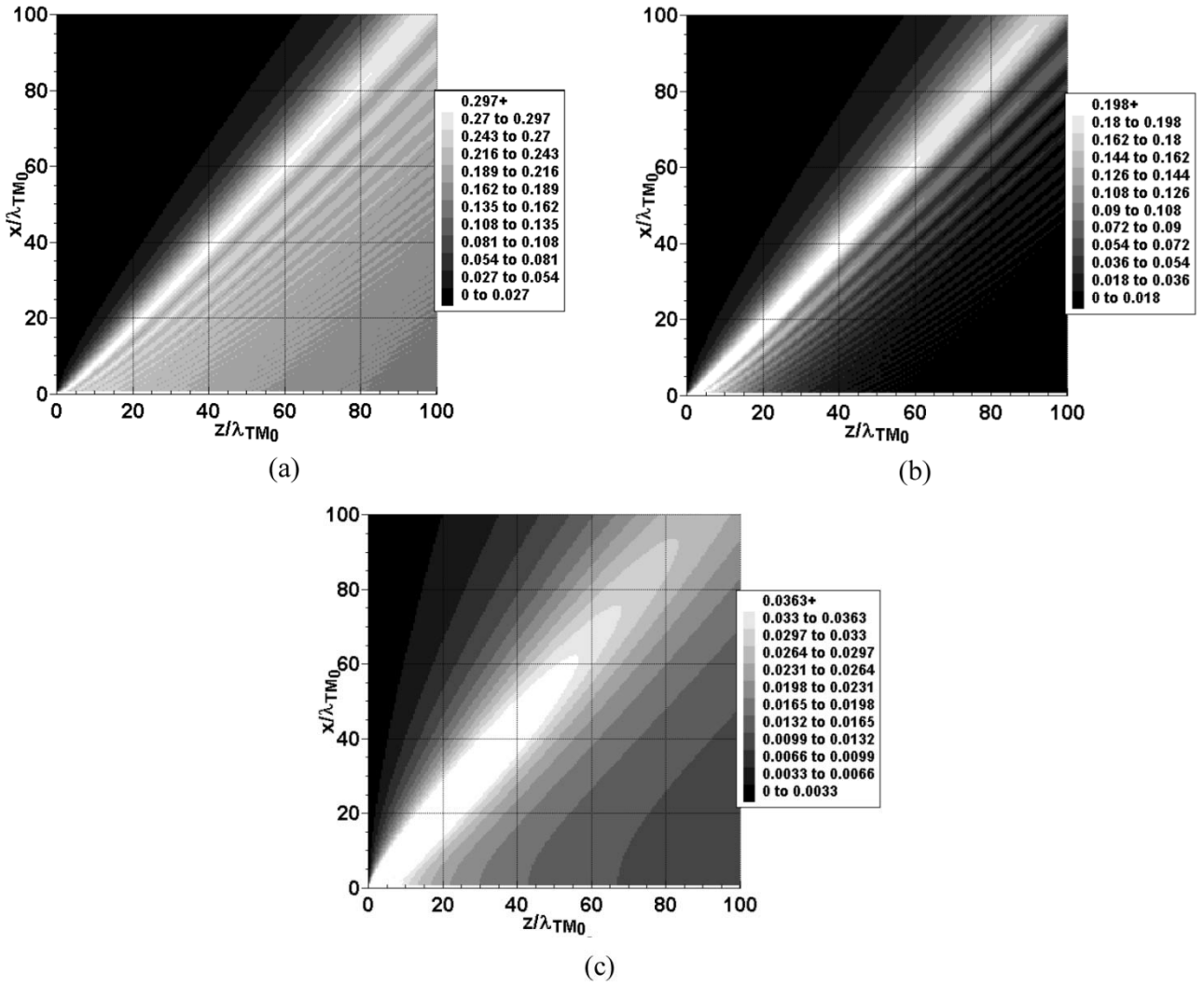


Fig. 2. Vertical component of the normalized leaky-mode electric field for $\phi_0 = 50°$. (a) $\bar{\alpha}_z = 0.001$. (b) $\bar{\alpha}_z = 0.01$. (c) $\bar{\alpha}_z = 0.1$.

away from the shadow boundary. This feature is not predicted by GO. This oscillation is the result of interference between the leakage field and the "source discontinuity radiation field" [12], the field that physically arises because of the discontinuity in the derivative of the current at $z' = 0$ in (4). The source discontinuity radiation spreads radially from the source location, attenuating as $1/\sqrt{\rho}$ with a phase variation of $\exp(-jk_{\mathrm{TM}_0}\rho)$. The GO field has a phase variation of $\exp(-j(\beta_z z + \beta_x x))$ within the lit region, where $\beta_z = \mathrm{Re}(k_z) \approx k_{\mathrm{TM}_0}\cos\phi_0$ and $\beta_x = \mathrm{Re}(k_x) \approx k_{\mathrm{TM}_0}\sin\phi_0$. This simple explanation predicts the periodicity of the oscillations seen in Fig. 2(a).

The results in Fig. 2(b) demonstrate that when $\bar{\alpha}_z$ is increased to 0.01, the overall field strength is decreased, and the radiation shape becomes more focused along the leakage angle. That is, more of a "beam" exists in the near field. This is because the field decreases more rapidly within the lit region in the direction perpendicular to the leakage boundary. Further increase in $\bar{\alpha}_z$ yields radiation that is diffuse with no well-defined lit region or beam, as shown in Fig. 2(c), which is characteristic of radiation from a more localized current near the source.

The trends in Fig. 2 highlight some general properties associated with different leaky-mode attenuations constants. For smaller values of $\bar{\alpha}_z$, the leakage field is more nearly uniform in the lit region and very weak in the shadow region. The gradient of the field in the shadow region, along a direction perpendicular to the shadow boundary, is large for $\bar{\alpha}_z = 0.001$, creating an abrupt decay of the field past the shadow boundary. The gradient within the lit region is fairly small (GO predicts that this gradient should become smaller as $\bar{\alpha}_z$ decreases). As $\bar{\alpha}_z$ is increased, this gradient becomes smaller in the shadow region and larger in the lit region, eventually blurring the definition of the lit region. The field magnitude is also changing more rapidly along the leakage angle direction as $\bar{\alpha}_z$ increases.

## III. Leaky-Mode Poynting Vector

The leaky-mode radiation field can be further understood by investigating the associated power flow. This power flow can be calculated using the time-average Poynting vector

$$\langle \mathbf{S} \rangle = \frac{1}{2}\mathrm{Re}\{\mathbf{E} \times \mathbf{H}^*\}. \tag{8}$$

The magnetic field associated with the radiation field calculated in (5) is determined from the electric field in (5) using Faraday's

law (see the Appendix for details). The final expression for the Poynting vector of the leaky-mode radiation field is written as

$$\begin{aligned}\langle \mathbf{S} \rangle = &- \frac{|A_N|^2}{2\omega\mu\lambda_{\mathrm{TM}_0}} \\ &\times \mathrm{Re}\left\{ j\hat{\mathbf{x}} \int_{-\infty}^{+\infty} e^{-j\bar{k}_z 2\pi|\bar{z}'|} g(\bar{x},\bar{z},\bar{z}')d\bar{z}' \right. \\ &\quad \times \left( \int_{-\infty}^{+\infty} e^{-j\bar{k}_z 2\pi|\bar{z}'|} \frac{\partial g(\bar{x},\bar{z},\bar{z}')}{\partial \bar{x}} d\bar{z}' \right)^* \\ &\quad + j\hat{\mathbf{z}} \int_{-\infty}^{+\infty} e^{-j\bar{k}_z 2\pi|\bar{z}'|} g(\bar{x},\bar{z},\bar{z}')d\bar{z}' \\ &\quad \left. \times \left( \int_{-\infty}^{+\infty} e^{-j\bar{k}_z 2\pi|\bar{z}'|} \frac{\partial g(\bar{x},\bar{z},\bar{z}')}{\partial \bar{z}} d\bar{z}' \right)^* \right\} \quad (9)\end{aligned}$$

where

$$g(\bar{x},\bar{z},\bar{z}') = H_1^{(2)}(2\pi\bar{\rho}')\cos\phi'. \quad (10)$$

Fig. 3 shows a vector plot of the power flow for $\bar{\alpha}_z = 0.001$ and $\phi_0 = 50°$. Fig. 3 illustrates the close correlation between power flow and the amplitude of the field, as shown in Fig. 2. The vector plot shows that the time-average power flow is directed away from the source and along the direction of leakage. It is also evident (although not shown explicitly here) by closely examining Fig. 3 that magnitude plots of the power are very similar to the field plots such as those shown in Fig. 2. Hence, the field plots give indications not only of the radiated field intensity, but also of the power flow into the surrounding background structure.

Fig. 3(b) shows an expanded view of the power flow near the source. From this expanded view, it is evident that the strongest radiation does not emanate directly from the source at $z = 0$. Instead, there is an *effective point of radiation* that is displaced from the source along the $z$-axis. This effective point of radiation is a direct result of the interference between the source discontinuity radiation and the infinite-line leaky-mode field. This phenomenon will be explained in more detail in the following section.

Fig. 4 shows the magnitude of the normalized leaky-mode field plotted for $\phi_0 = 10°$ and $\bar{\alpha}_z = 0.001, 0.01, 0.1$, respectively. Examining these three plots, it is clear that the general conclusions presented for Fig. 2 based on $\bar{\alpha}_z$ continue to hold. At this lower leakage angle (larger $\bar{\beta}_z$), the normalized leaky-mode radiation field is stronger compared to the higher angle of leakage shown in Fig. 2. This is due in part to the $\cos\phi'$ term in (5). However, as the leakage angle gets closer to end-fire (the leakage angle tends to zero), the leakage beam diffuses. The larger $\bar{\alpha}_z$ becomes, the faster the leakage beam diffuses near end-fire. A low leakage angle also leads to a leakage beam that is partially collapsed into the strip, creating an effective point of radiation that lies much further out along the $z$-axis. Although further results are not shown here, the field strength and effective point of radiation trends continue for other values of $\bar{\beta}_z$. The normalized field strength generally decreases and the effective point of radiation lies closer to the source as $\bar{\beta}_z$ decreases (or $\phi_0$ increases).

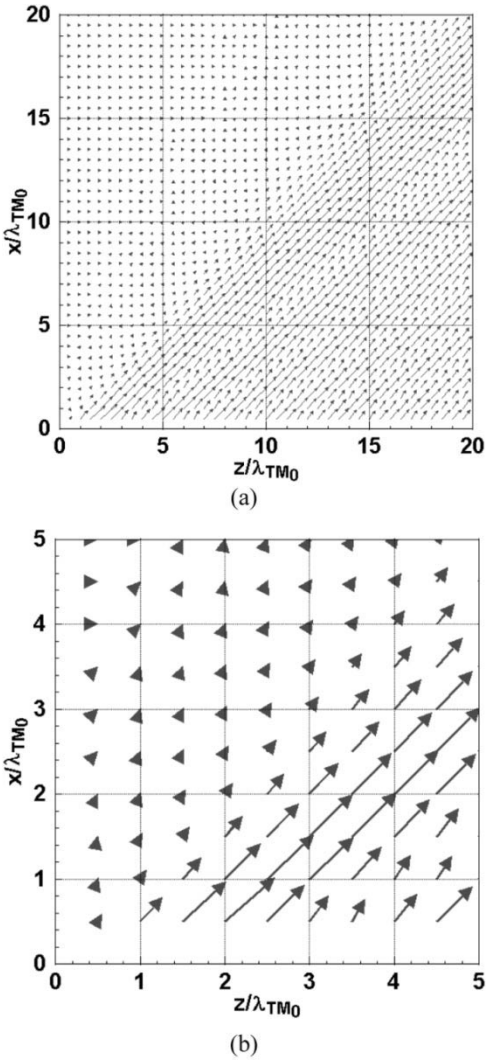


Fig. 3. Normalized Poynting vector for the leaky-mode field for $\phi_0 = 50°$ and $\bar{\alpha}_z = 0.001$ for: (a) $0 \le \bar{x}, \bar{z} \le 20$, and (b) $0 \le \bar{x}, \bar{z} \le 5$.

## IV. Effective Point of Radiation

The effective point of radiation is the point along the strip where the maximum magnitude of the leaky-mode radiation field is located. This is the location where the two radiation mechanisms associated with the leaky-mode (the source-discontinuity radiation and infinite-line leaky-mode field) constructively interfere. The effective point of radiation is not at $z = 0$, but is shifted along the line away from the source. As seen in Figs. 2 and 3, the radiation beam appears to emanate from this point. Hence, when plotting the field versus $z$ for a fixed $x$ that is close to the strip, the maximum field occurs at some value $z_M$ larger than zero.

To further investigate this interesting interference effect, the field close to the strip is assumed to be the sum of a GO leaky-mode field and a source-discontinuity field (which is a radial field that emanates from the source location). This

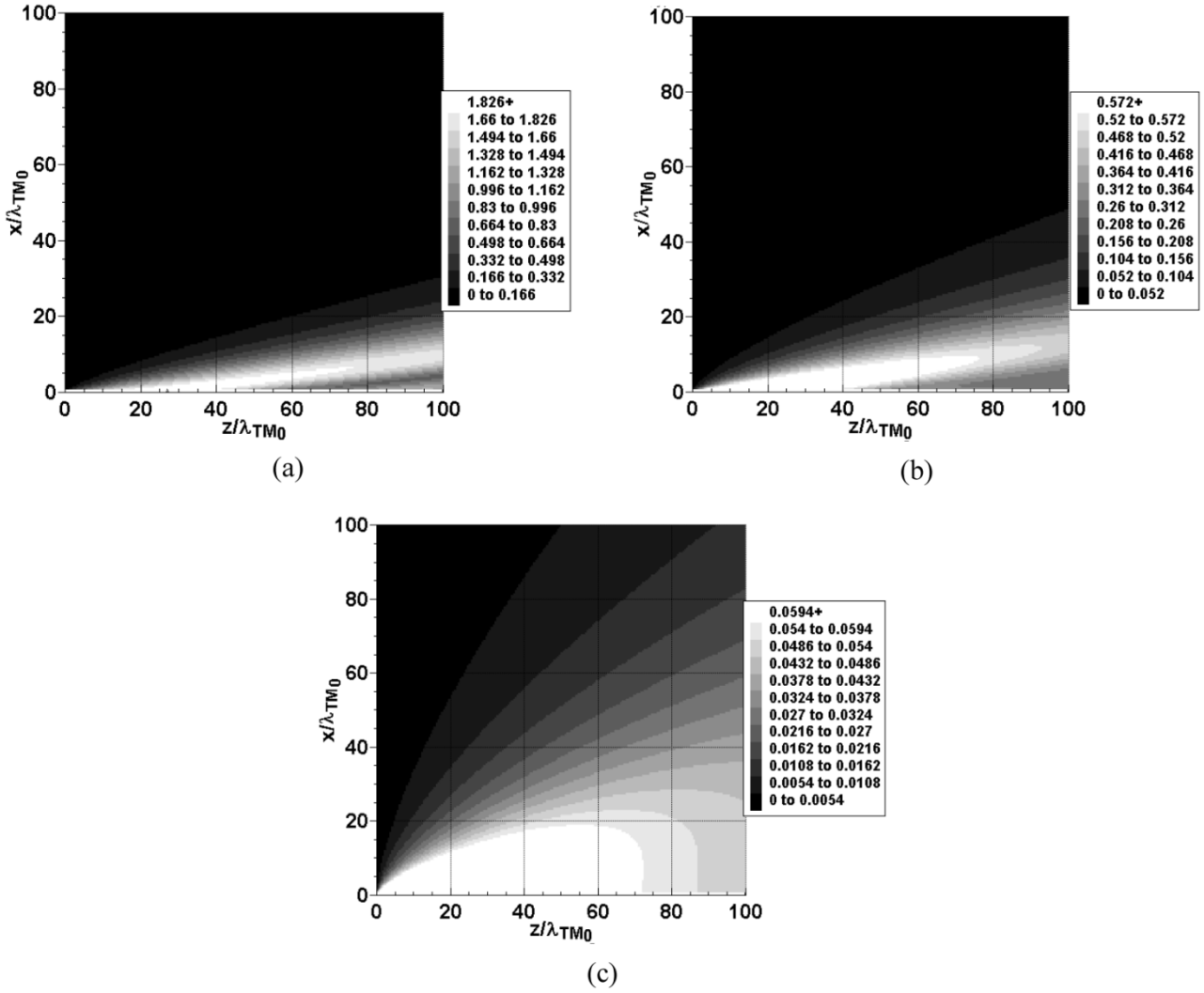


Fig. 4. Vertical component of the normalized leaky-mode electric field for $\phi_0 = 10°$. (a) $\bar{\alpha}_z = 0.001$. (b) $\bar{\alpha}_z = 0.01$. (c) $\bar{\alpha}_z = 0.1$.

approximation should be accurate for very small $\bar{\alpha}_z$. Approximating the Hankel function of the source discontinuity field using its large-argument asymptotic form [15]

$$H_\nu^{(2)}(\zeta) \sim \sqrt{\frac{2}{\pi\zeta}} e^{-j\left(\zeta - \frac{\nu\pi}{2} - \frac{\pi}{4}\right)} \tag{11}$$

this field can be written as

$$E_y \approx A_1 e^{-jk_z z} e^{-jk_x x} + \frac{A_2}{\sqrt{\rho}} e^{-jk_{\mathrm{TM}_0}\rho} \tag{12}$$

where $A_1$ and $A_2$ are some complex constants. Assuming that $x = x_0$ is fixed and small, and making use of (7), (12) can be simplified to

$$E_y \approx |A_3| e^{j\phi_3} e^{-jk_{\mathrm{TM}_0}\cos(\phi_0)z} + \frac{|A_2|}{\sqrt{z}} e^{j\phi_2} e^{-jk_{\mathrm{TM}_0}z} \tag{13}$$

where $A_3 = A_1 e^{-jk_x x_0}$ and $\phi_3$ and $\phi_2$ are the phases of $A_3$ and $A_2$. Hence, the location of the maximum field, when plotted along the strip, will occur at $\bar{z} = \bar{z}_M$ when

$$\bar{z}_M = \frac{A_0}{1 - \cos(\phi_0)} \tag{14}$$

where

$$A_0 = \frac{\phi_2 - \phi_3}{2\pi}. \tag{15}$$

Equation (14) predicts that the effective point of radiation is not, in general, at the origin, and that the location shifts further away from the origin as the leakage angle decreases. Results for the effective point of radiation have been numerically calculated for $\bar{\alpha}_z = 0.001, 0.01,$ and $0.1$. The results for these cases and the theoretical approximation in (14) are presented in Fig. 5. Since $A_0$ is not known numerically, the numerically calculated data is equated with the theoretical approximation (14) at $\phi_0 = 90°$ to find the value of $A_0$. Fig. 5 shows that, for all of the cases, the effective point of radiation is increasing with decreasing leakage angle; however, the rate of increase is much more dramatic as $\bar{\alpha}_z$ becomes smaller. The theoretical approximation agrees well with the numerically calculated data for large leakage angles, but the agreement fades as the leakage angles become smaller (even though the general shapes of the curves are very similar). For small leakage angles (near $\phi_0 = 0$), the effective point of radiation converges to a fixed value. This stabilizing effect is

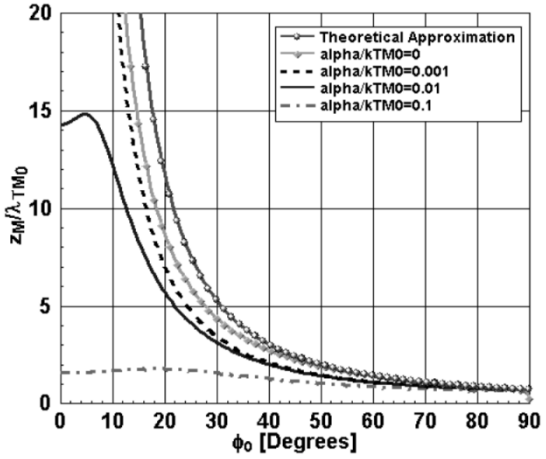


Fig. 5. Effective point of radiation ($\bar{z}_M = z_M/\lambda_{\mathrm{TM}_0}$) for the normalized leaky-mode electric field versus approximate leakage angle $\phi_0$.

more pronounced for larger $\bar{\alpha}_z$, as seen when comparing the curves for $\bar{\alpha}_z = 0.1$ and 0.01. This is probably due to the fact that, for larger $\bar{\alpha}_z$, the leakage beam diffuses more rapidly as the leakage angle approaches end fire.

## V. GO and Far-Field Patterns

### A. GO Field

The GO field is that predicted by "ray optics" theory, and should be valid in the limit that $\bar{\alpha}_z \to 0$ and the distance from the line increases (so that source-discontinuity radiation becomes small). The magnitude of the GO field is written as [12]

$$\left|E_y^{\mathrm{GO}}(\bar{x},\bar{z})\right| = \frac{|A_N|}{\pi}\cot(\phi_0) \times \begin{cases} e^{-\bar{\alpha}_z 2\pi|\bar{z}|}e^{-\bar{\alpha}_x 2\pi|\bar{x}|}, & (\bar{x},\bar{z}) \text{ in the lit region} \\ 0, & \text{otherwise} \end{cases} \tag{16}$$

where $\bar{\alpha}_x$ is negative for a leaky mode. Since only $\bar{\alpha}_z$ is specified in the calculations, it is convenient to eliminate $\bar{\alpha}_x$ from (16). The wavenumbers are related by

$$\bar{k}_x^2 + \bar{k}_z^2 = \left(\bar{\beta}_x - j\bar{\alpha}_x\right)^2 + \left(\bar{\beta}_z - j\bar{\alpha}_z\right)^2 = 1. \tag{17}$$

By taking the imaginary part of (17), it is seen that

$$\bar{\beta}_x\bar{\alpha}_x = -\bar{\beta}_z\bar{\alpha}_z. \tag{18}$$

Assuming that the attenuation constants are small, $\bar{\beta}_x$ and $\bar{\beta}_z$ can both be related to the leakage angle as in (7) and, hence,

$$\bar{\alpha}_x = -\bar{\alpha}_z\cot(\phi_0). \tag{19}$$

Using these approximations and converting to cylindrical coordinates, the GO field in the region $z > 0$ is given by

$$\left|E_y^{\mathrm{GO}}(\bar{x},\bar{z})\right| = \frac{|A_N|}{\pi} \times \cot(\phi_0)\begin{cases} e^{\bar{\alpha}_z 2\pi\bar{\rho}|\sin(\phi)|[\cot(\phi_0)-|\cot(\phi)|]}, & |\phi| \le |\phi_0| \\ 0, & \text{otherwise.} \end{cases} \tag{20}$$

### B. Far-Field Pattern

The far-field pattern is obtained by evaluating (5) at large distances from the source, where the Hankel function in (5) is approximated by its asymptotic form [given in (11)] for $\bar{\rho} \to \infty$. Using these far-field approximations, the infinite integration is evaluated in closed form. Hence, the expression for the magnitude of the far field is written as

$$\left|E_y^{FF}(\bar{x},\bar{y},\bar{z})\right| = |A_N|\frac{|\cos(\phi)|}{2\pi^2\sqrt{\bar{\rho}}}\left|\frac{1}{\bar{k}_z - \cos(\phi)} + \frac{1}{\bar{k}_z + \cos(\phi)}\right|. \tag{21}$$

### C. Results

Fig. 6 shows the GO, far-field, and numerically exact (henceforth referred to as "exact") patterns for $\bar{\alpha}_z = 0.01$ and $\phi_0 = 50°$ for $\bar{\rho} = 1, 10, 100, 1000$. At $\bar{\rho} = 1$, there is no agreement between the GO, far-field, and exact patterns. The lack of agreement is easily explained in this case since the distance from the source is too small for the far-field expressions to be accurate, and also too small for the GO field to be accurate since, at this small distance, the dominant part of the radiation from the leaky mode is source-discontinuity radiation. At $\bar{\rho} = 10$, the agreement between GO and the exact leaky-mode radiation field is good. The overall shape of the exact leaky-mode radiation field agrees well with the shape of the GO field. The oscillations in the exact leaky-mode radiation field correspond to the interference between a GO leaky-mode field and a source discontinuity radiation field. Past the shadow boundary, there is only the source discontinuity radiation, thus, the exact leaky-mode radiation field is smooth and decays monotonically. In the shadow region, the far field is beginning to agree with the exact field for large observation angles ($\phi \ge 65°$). At $\bar{\rho} = 100$, the agreement between GO and the exact leaky-mode field is beginning to break down; however, the agreement with the far-field pattern is becoming much better, especially in the shadow region. Agreement between the exact and far-field patterns for the leaky mode is excellent at $\bar{\rho} = 1000$ for all observation angles. At this distance, the exact leaky mode is very well described by its far-field pattern and the GO pattern (which has the appearance of a sharp spike) has no agreement at all with the exact leaky-mode radiation field. This general behavior is typical of all leaky-mode radiation fields. The exact fields generally agree well with the GO fields within a range of $\bar{\rho}$, the size of which depends primarily on $\bar{\alpha}_z$. In general, the agreement between the exact and GO fields improves as $\bar{\alpha}_z$ decreases. The larger $\bar{\alpha}_z$, the smaller the region of agreement since the transition from

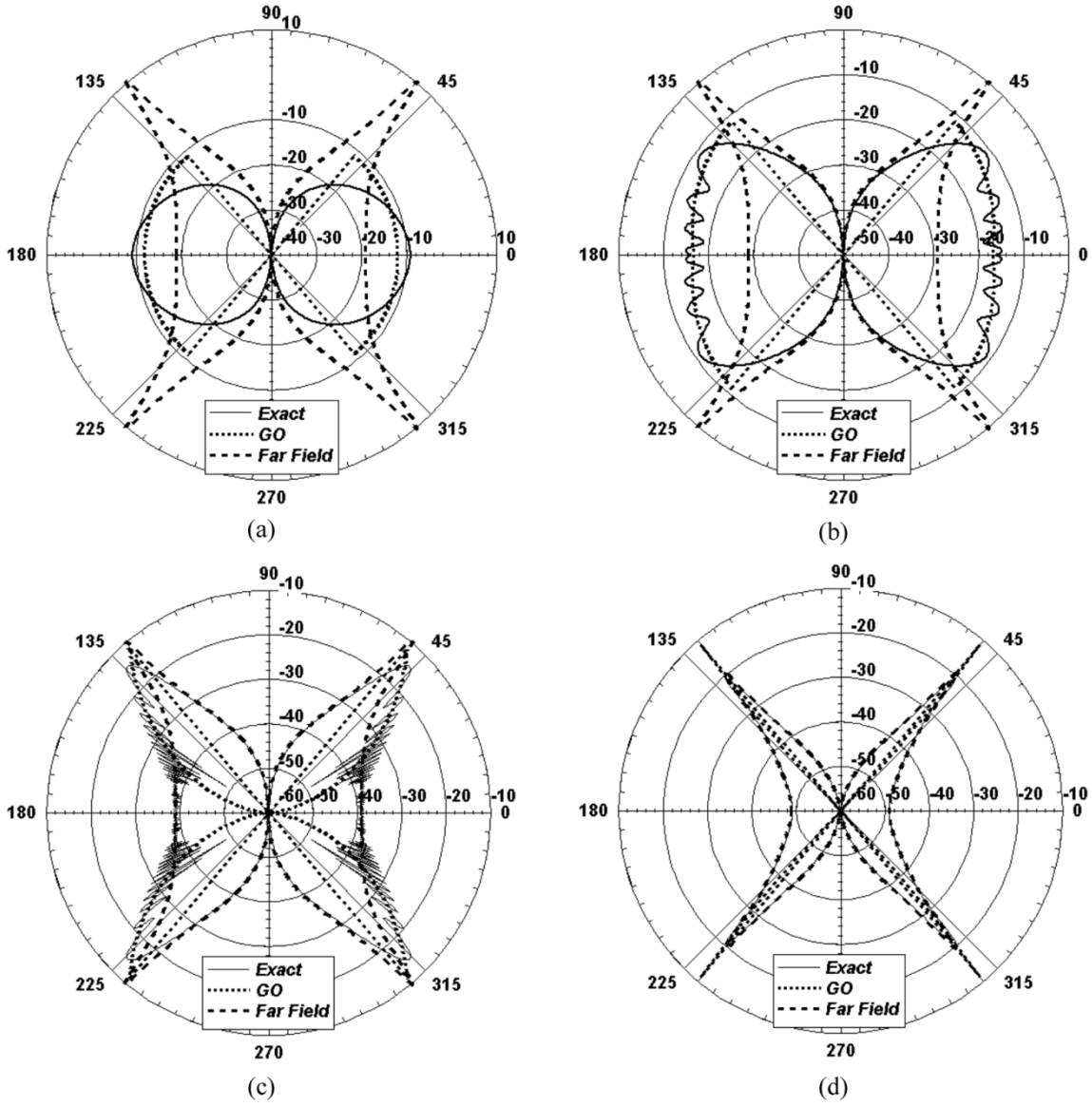


Fig. 6. Vertical component of the normalized leaky-mode electric field compared with GO and far-field patterns (in decibels) for $\bar{\alpha}_z = 0.01$ and $\phi_0 = 50°$. (a) $\bar{\rho} = 1$. (b) $\bar{\rho} = 10$, (c) $\bar{\rho} = 100$. (d) $\bar{\rho} = 1000$.

the near to far field occurs more quickly. If $\bar{\alpha}_z$ gets too large, the exact field never agrees well with the GO field for any value of $\bar{\rho}$. The region of agreement between the exact and GO fields (the range of $\bar{\rho}$ over which agreement occurs) is also smaller as the leakage angle decreases. This is because the leakage field becomes more diffuse as the leakage angle decreases. Comparisons of the far-field pattern and the exact leaky-mode radiation field show that agreement between these fields is good for large $\bar{\rho}$. The exact leaky-mode radiation field for larger values of $\bar{\alpha}_z$ converges to the far-field pattern at smaller values of $\bar{\rho}$ since larger values of $\bar{\alpha}_z$ lead to smaller effective lengths of radiating current.

One interesting conclusion is that, for small values of $\bar{\alpha}_z$ and small leakage angles, the peak value of the radiation field actually increases for small $\bar{\rho}$, as $\bar{\rho}$ gets larger. Eventually, however, the value of the peak field decreases with increasing $\bar{\rho}$. For larger values of $\bar{\alpha}_z$, the peak value of the field decreases with $\bar{\rho}$ for all $\bar{\rho}$. When $\bar{\alpha}_z$ is small, there is a range of $\bar{\rho}$ for which the peak value of the field changes very slowly with $\bar{\rho}$. This is as expected from GO (which predicts that the peak value of the field is at the shadow boundary, and is independent of the distance $\bar{\rho}$).

## VI. Radiation From a Nonphysical Leaky Mode

A nonphysical leaky mode is a mode that has a complex wavenumber, but is a slow wave with respect to $k_{\mathrm{TM}_0}$ ($\bar{\beta}_z > 1$). This type of mode becomes important when a structure is operated at a frequency in the "spectral-gap region" [14], [16]. The spectral-gap region is the frequency span where a leaky mode exists, but is nonphysical because it is a slow wave. In this frequency region, a nonphysical leaky-mode field can still be significant, and can even dominate the total radiation field, particularly when no other physical leaky mode is present [17].

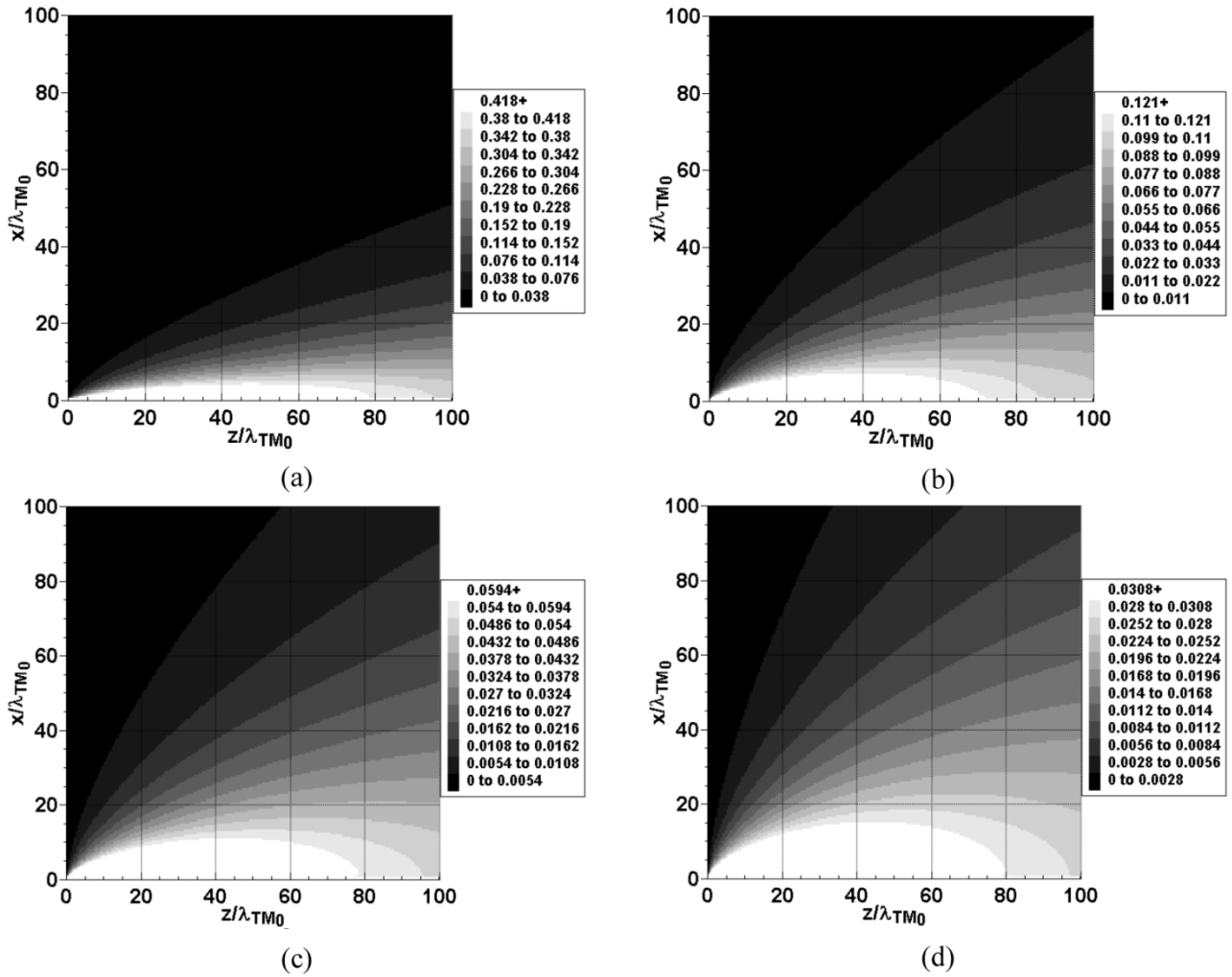


Fig. 7. Vertical component of the normalized leaky-mode electric field for a nonphysical leaky mode for $\bar{\alpha}_z = 0.01$. (a) $\bar{\beta}_z = 1.01$. (b) $\bar{\beta}_z = 1.05$. (c) $\bar{\beta}_z = 1.1$. (d) $\bar{\beta}_z = 1.2$.

Fig. 7 shows nonphysical leaky-mode radiation patterns for $\bar{\alpha}_z = 0.01$ and $\bar{\beta}_z = 1.01, 1.05, 1.10,$ and $1.20$. All of the patterns shown in Fig. 7 show an end-fire type of radiation field. A strongly directed beam is not produced, but instead, the radiation pattern is rather diffuse and gets more diffuse as the value of $\bar{\beta}_z$ increases within the spectral-gap region.

## VII. Results for Different Source Excitations

Thus far, results for the leaky-mode radiation field have been plotted assuming a bi-directional even leaky-mode current, as would result from the gap voltage source shown in Fig. 1. In practice, there are three different current distributions that could occur on a given planar transmission-line structure, i.e., a bi-directional even-mode current, bi-directional odd-mode current, and a unidirectional current on a semi-infinite line. Results are presented below for leaky-mode currents with these different distributions.

### *A. Unidirectional Current*

Unidirectional current excitation occurs when a current is excited in one direction on a semi-infinite line. On a planar transmission line, this type of current excitation occurs when the line is fed from below using a coaxial probe or a via feed. A typical configuration for this type of feed is shown in Fig. 8(a). Fig. 9(a) shows the magnitude of the radiation fields associated with a unidirectional leaky-mode current for $\bar{\alpha}_z = 0.1$ and $\phi_0 = 50°$. The current is excited by a source at $z = 0$ and extends in the $+z$-direction. From Fig. 9(a), it is readily seen that the radiation field is much stronger in the positive $z$ region due to a strong contribution from the leaky-mode current. In the negative $z$ region, the radiation field is weak, associated primarily with source discontinuity radiation.

### *B. Bi-Directional Even-Mode Current*

Bi-directional even-mode current excitation occurs when a current is excited equally in both directions with the same phase. This type of current excitation corresponds to a gap voltage source, as shown in Fig. 1. Fig. 8(b) illustrates how such an excitation could take place in a realistic planar transmission-line package using an end-launch connector. This configuration yields the bi-directional even-mode excitation through image theory since the planar transmission line is fed at the end and a metallic plane (modeled as infinite) supports the feed probe. Fig. 9(b) shows the radiation field due to this

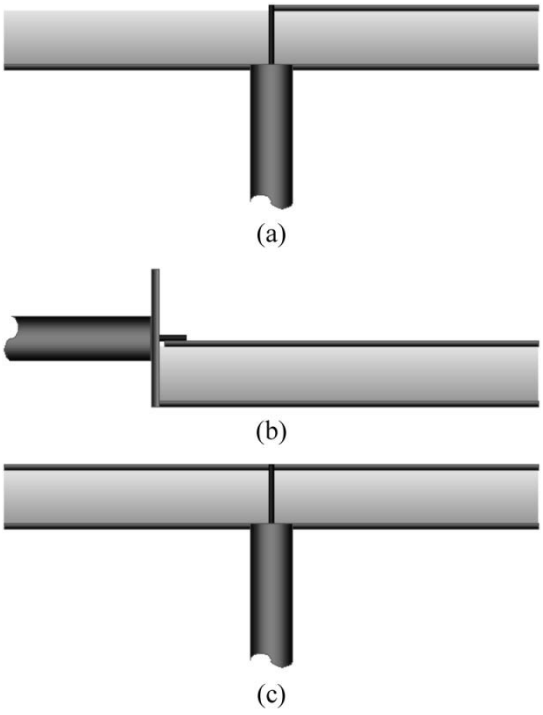


Fig. 8. Three different source excitations of the printed circuit line. (a) Probe feed for a semi-infinite line, which produces a unidirectional current. (b) End-launch coaxial connector feeding a semi-infinite line, which, by image theory, produces a bi-directional even-mode current. (c) Vertical probe connector for an infinite line, which produces a bi-directional odd-mode current.

type of leaky-mode current for $\bar{\alpha}_z = 0.1$ and $\phi_0 = 50°$. Since the current is excited equally in both directions with the same phase, this case is like the superposition of two oppositely directed unidirectional cases that are $180°$ out of phase from each other. The result is a symmetric field around the source with each side being slightly weaker in magnitude near the source than the field obtained for the unidirectional case. This weakening of the field is due to the even-mode nature of the strip current, which causes the radiation field to have a null at $\phi = 90$.

### C. Bi-Directional Odd-Mode Current

Bi-directional odd-mode current excitation occurs when a current is excited equally in both directions with the opposite phase. This type of current excitation corresponds to a vertical current source such as a coaxial probe or via feed that makes contact with an infinite line. Fig. 8(c) illustrates how such an excitation could take place in a realistic planar transmission-line circuit. Fig. 9(c) shows the radiation field due to this type of leaky-mode current for $\bar{\alpha}_z = 0.1$ and $\phi_0 = 50°$. Since the current is excited equally in both directions with opposite phase, this case is basically the superposition of two oppositely directed unidirectional cases. The result is a symmetric field around the source with each side being slightly stronger in magnitude near the source than the field obtained for the unidirectional case. The strengthening of the field is due to constructive interference that occurs near $\phi = 90$ from radiation due to the currents on the opposite side of the source (as opposed to the cancellation that occurs with the even-mode excitation).

## VIII. Practical Example: Covered Microstrip

An example is presented in Figs. 10 and 11 to aid in explaining how the normalized leaky-mode fields can be applied toward a practical structure. Fig. 10 shows the dispersion plot for a covered microstrip structure with equally dimensioned strip width, substrate thickness, and cover height above the substrate $(W = h = h_c)$ and relative permittivity of the substrate $\varepsilon_r = 2.2$. Fig. 11 shows the field plot for this structure at a normalized frequency of $h/\lambda_0 = 0.1$. The leaky-mode field for this structure is calculated using the normalized radiation formula (5) with knowledge of the leaky-mode wavenumber $k_z = (1.132 - j0.1036)k_0$ and the $\mathrm{TM}_0$ wavenumber of the background structure $k_{\mathrm{TM}_0} = 1.191k_0$ $(\lambda_{\mathrm{TM}_0} = 0.8396\lambda_0)$ obtained from Fig. 10. Hence, the normalized wavenumber is $\bar{k}_z = 0.9505 - j0.08699$. The unnormalized field for this structure can be calculated by evaluating $A_N$. For this covered microstrip structure, $A_N = -64.47 + j1.008$ V/m for $y$ at the ground plane. The resulting unnormalized leaky-mode field for this example structure is shown in Fig. 11(a). The shape of this leaky-mode field is consistent with the earlier results shown for large $\bar{\alpha}_z$ and small leakage angle. The leakage field is diffuse with no well-defined beam. By examining the data used for Fig. 11(a), the effective point of radiation for this example is calculated to be $z_M = 1.75\lambda_0 = 2.08\lambda_{\mathrm{TM}_0}$. This agrees well with the results shown in Fig. 5. Fig. 11(b) shows the *total field* for this example structure that is calculated from the *total current* excited on the structure for comparison [13], [14]. Comparing Fig. 11(a) and (b), it is readily seen that the leaky-mode field is a dominant contributor to the total field. However, it is important to note that the shape of the total field does not completely match that of the leaky-mode field due to the contributions of the bound-mode source-discontinuity radiation and the radiation from to the remainder of the continuous spectrum [13], [14].

## IX. Conclusions

It has been shown that the field radiated by a leaky mode that is excited by a source on an infinite or semi-infinite printed-circuit transmission line can be represented in a general unified manner. That is, after proper normalization, the results apply to the radiation field from a leaky mode on any type of printed-circuit structure. The leaky mode is assumed to be excited by a source at the center of an infinite line, which produces either an even or an odd current distribution about the source. Alternatively, the leaky-mode current may be in the form of a unidirectional current mode on a semi-infinite line that is excited by a source at the end of the line. For all cases, the leaky mode is assumed to only radiate into the fundamental $\mathrm{TM}_0$ mode of the background structure.

The results show that a well-defined leakage region is produced when the leakage constant is small and the leakage angle is not too close to zero. As the leakage constant becomes smaller, the radiation field agrees better with an approximate closed-form GO field, which physically describes the leakage

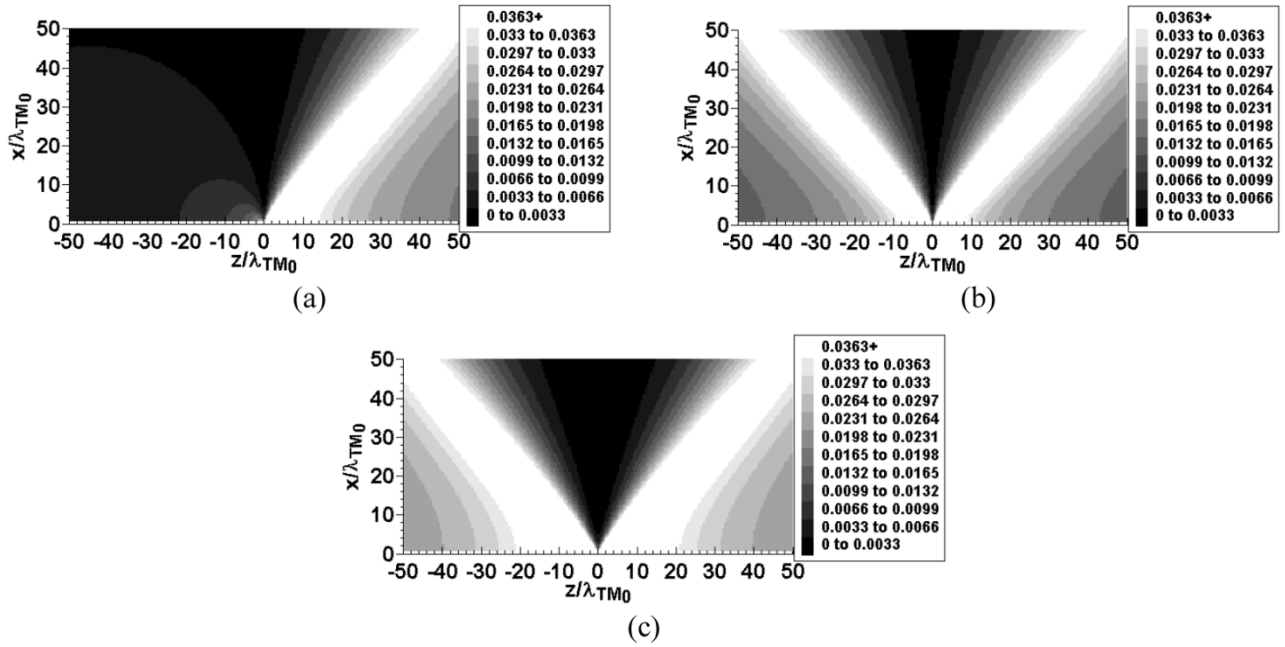


Fig. 9. Vertical component of the normalized leaky-mode electric field for $\bar{\alpha}_z = 0.1$, $\phi_0 = 50°$. (a) Unidirectional current. (b) Bi-directional even-mode current. (c) Bi-directional odd-mode current.

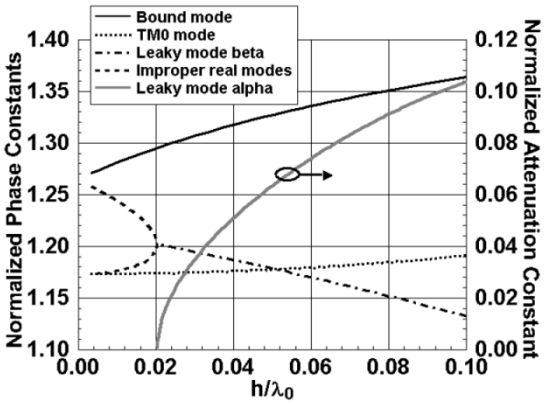


Fig. 10. Dispersion plot showing the normalized phase constant $\beta_z/k_0$ and normalized attenuation constant $\alpha_z/k_0$ of the leaky mode versus normalized frequency $h/\lambda_0$ for a covered microstrip transmission line ($W = h = h_c$ and $\varepsilon_r = 2.2$). Also shown is normalized phase constant $\beta_z/k_0$ for the bound mode and the normalized phase constant $k_{\mathrm{TM}_0}/k_0$ for the $\mathrm{TM}_0$ mode.

field in terms of "rays" that carry power away from the line. This simple model predicts a field that is constant along the lines of leakage within the leakage (or lit) region, and essentially zero in the shadow region. The exact radiation field can be interpreted as consisting of a GO leakage field together with a source-discontinuity field, which is essentially a radially propagating field that emanates form the source location. The source-discontinuity field is strong for distances close to the source so the GO field does not agree well with the exact field near the source or for large distances from the source. However, the GO field agrees quite well with the exact field over a significant range of moderate distances from the source, when the leakage constant is sufficiently small. For large distances from the source, the exact field agrees well with a closed-form far-field approximate formula for the radiation field of the leaky mode.

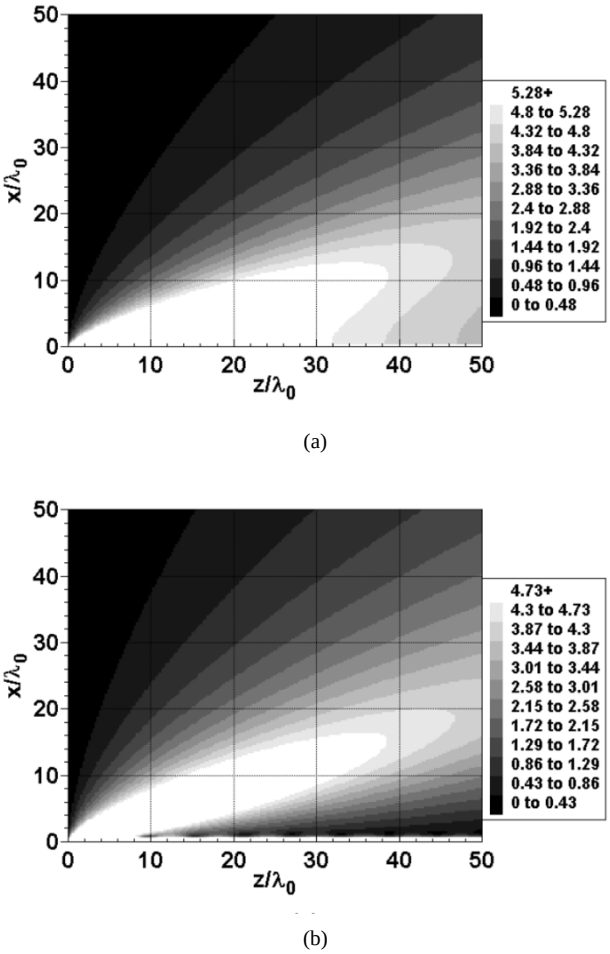


Fig. 11. (a) Leaky-mode electric field and (b) total electric field for the structure of Fig. 10 at $h/\lambda_0 = 0.1$ for a 1-V gap (bi-directional even-mode current) source excitation. The unnormalized field is plotted in volts per meter.

Results for the power flow in the leaky-mode radiation field were also presented, and these correlate well with the results for the radiation field intensity, showing power flow primarily in the direction of leakage, as expected. Interestingly, the power flow does not typically appear to emanate from the source region, but instead from a region that is displaced along the line from the source, which has been termed the "effective point of radiation." A simple approximate formula for predicting the location of this point has been derived.

The case of a nonphysical leaky mode (a slow wave with respect to the background mode into which radiation is occurring) was also investigated. It was shown that the radiation field from such a leaky mode is fairly diffuse and becomes more so as the phase constant increases and the mode correspondingly becomes less physical.

It was shown that the radiation field from all three types of current distributions (bi-directional even-mode and odd-mode, and unidirectional) are very similar in the forward leakage region (the leakage region for $z > 0$). The even- and odd-mode bi-directional cases have a symmetrical radiation field, while the unidirectional case produces a strong leakage field in only the forward direction and has a weak field in the backward region.

A specific example for one particular practical structure (a covered microstrip structure exited by a gap source) was used to illustrate the general method, showing how the fields of the leaky mode on this particular structure could be predicted based on the known dispersion curve.

## APPENDIX

Since only the $\hat{\mathbf{y}}$ component of the electric field is of interest, the time-average Poynting vector [see (8)] simplifies to

$$\langle \mathbf{S} \rangle = \frac{1}{2}\mathrm{Re}\Big\{E_y H_z^* \hat{\mathbf{x}} - E_y H_x^* \hat{\mathbf{z}}\Big\}. \tag{A1}$$

From Maxwell's equations, the $\hat{\mathbf{x}}$ and $\hat{\mathbf{z}}$ components of the magnetic field are given by

$$H_x(\bar{x},\bar{y},\bar{z}) = \frac{A_N}{j\omega\mu\lambda_{\mathrm{TM}_0}} \int_{-\infty}^{+\infty} e^{-j\bar{k}_z 2\pi|\bar{z}'|} \frac{\partial g(\bar{x},\bar{z},\bar{z}')}{\partial \bar{z}} d\bar{z}' \tag{A2}$$

and

$$H_z(\bar{x},\bar{y},\bar{z}) = -\frac{A_N}{j\omega\mu\lambda_{\mathrm{TM}_0}} \int_{-\infty}^{+\infty} e^{-j\bar{k}_z 2\pi|\bar{z}'|} \frac{\partial g(\bar{x},\bar{z},\bar{z}')}{\partial \bar{x}} d\bar{z}'. \tag{A3}$$

Hence, substituting (5), (A2), and (A3) into (A1), the Poynting vector can be written in normalized form as

$$\begin{aligned}\langle \mathbf{S} \rangle = &-\frac{|A_N|^2}{2\omega\mu\lambda_{\mathrm{TM}_0}} \\ &\times \mathrm{Re}\left\{ j\hat{\mathbf{x}} \int_{-\infty}^{+\infty} e^{-j\bar{k}_z 2\pi|\bar{z}'|} g(\bar{x},\bar{z},\bar{z}')d\bar{z}' \right. \\ &\quad \times \left( \int_{-\infty}^{+\infty} e^{-j\bar{k}_z 2\pi|\bar{z}'|} \frac{\partial g(\bar{x},\bar{z},\bar{z}')}{\partial \bar{x}} d\bar{z}' \right)^* \\ &\quad + j\hat{\mathbf{z}} \int_{-\infty}^{+\infty} e^{-j\bar{k}_z 2\pi|\bar{z}'|} g(\bar{x},\bar{z},\bar{z}')d\bar{z}' \\ &\quad \left. \times \left( \int_{-\infty}^{+\infty} e^{-j\bar{k}_z 2\pi|\bar{z}'|} \frac{\partial g(\bar{x},\bar{z},\bar{z}')}{\partial \bar{z}} d\bar{z}' \right)^* \right\}\end{aligned} \tag{A4}$$

where

$$\frac{\partial g(\bar{x},\bar{z},\bar{z}')}{\partial \bar{z}} = \frac{H_1^{(2)}(2\pi\bar{\rho}')}{\bar{\rho}'}\left(1-\cos^2\phi'\right) + 2\pi\cos^2\phi' H_1^{(2)'}(2\pi\bar{\rho}') \tag{A5}$$

and

$$\begin{aligned}\frac{\partial g(\bar{x},\bar{z},\bar{z}')}{\partial \bar{x}} = &-\frac{\cos\phi'\sin\phi' H_1^{(2)}(2\pi\bar{\rho}')}{\bar{\rho}'} \\ &+2\pi\cos\phi'\sin\phi' H_1^{(2)'}(2\pi\bar{\rho}').\end{aligned} \tag{A6}$$

## REFERENCES


[1] H. Shigesawa, M. Tsuji, and A. A. Oliner, "Conductor-backed slot line and coplanar waveguide: Dangers and full-wave analysis," in *IEEE MTT-S Int. Microwave Symp. Dig.*, June 1988, pp. 199–202.

[2] T. Rozzi, F. Moglione, E. Marchionna, and M. Politi, "Hybrid modes, substrate leakage, and losses of slotline at millimeter-wave frequencies," *IEEE Trans. Microwave Theory Tech.*, vol. 38, pp. 1069–1078, Aug. 1990.

[3] J. Zehentner and J. Machac, "Properties of CPW in the sub-mm wave range and its potential to radiate," in *IEEE MTT-S Int. Microwave Symp. Dig.*, June 2000, pp. 1061–1064.

[4] J.-Y. Ke, I.-S. Tsai, and C. H. Chen, "Dispersion and leakage characteristics of coplanar waveguides," *IEEE Trans. Microwave Theory Tech.*, vol. 40, pp. 1970–1973, Oct. 1992.

[5] M. Tsuji, H. Shigesawa, and A. A. Oliner, "Simultaneous propagation of both bound and leaky modes on conductor-backed coplanar strips," in *IEEE MTT-S Int. Microwave Symp. Dig.*, June 1993, pp. 1295–1298.

[6] ——, "Printed-circuit waveguide with anisotropic substrates: A new leakage effect," in *IEEE MTT-S Int. Microwave Symp. Dig.*, June 1989, pp. 783–786.

[7] D. Nghiem, J. T. Williams, D. R. Jackson, and A. A. Oliner, "Leakage of the dominant mode on stripline with a small air gap," *IEEE Trans. Microwave Theory Tech.*, vol. 43, pp. 2549–2556, Nov. 1995.

[8] F. Mesa and R. Marqués, "Low frequency leaky regime in covered multilayered striplines," *IEEE Trans. Microwave Theory Tech.*, vol. 44, pp. 1521–1525, Sept. 1996.

[9] D. Nghiem, J. T. Williams, D. R. Jackson, and A. A. Oliner, "Existence of a leaky dominant mode on microstrip line with an isotropic substrate: Theory and measurements," *IEEE Trans. Microwave Theory Tech.*, vol. 44, pp. 1710–1715, Oct. 1996.

[10] F. Mesa, A. A. Oliner, D. R. Jackson, and M. J.Manuel J. Freire, "The influence of a top cover on the leakage from microstrip line," *IEEE Trans. Microwave Theory Tech.*, vol. 48, pp. 2240–2248, Dec. 2000.

[11] A. A. Oliner, "Leakage from higher modes on microstrip line with application to antennas," *Radio Sci.*, vol. 22, pp. 907–912, Nov. 1987.

[12] F. J. Villegas, D. R. Jackson, J. T. Williams, and A. A. Oliner, "Leakage fields from planar semi-infinite transmission lines," *IEEE Trans. Microwave Theory Tech.*, vol. 47, pp. 443–454, Apr. 1999.

[13] W. L. Langston, J. T. Williams, D. R. Jackson, and F. Mesa, "Spurious radiation from a practical source on a covered microstrip line," *IEEE Trans. Microwave Theory Tech.*, vol. 49, pp. 2216–2226, Dec. 2001.

[14] ——, "Frequency dependent characteristics of radiation from a voltage source on a covered microstrip line," in *IEEE MTT-S Int. Microwave Symp. Dig.*, June 2002, pp. 949–952.

[15] M. Abramowitz and I. A. Stegun, *Handbook of Mathematical Functions With Formulas, Graphs, and Mathematical Tables*. Boulder, CO: Nat. Bureau of Standards, 1964.

[16] P. Lampariello, F. Frezza, and A. A. Oliner, "The transition region between bound-wave and leaky-wave ranges for a partially dielectric-loaded open guiding structure," *IEEE Trans. Microwave Theory Tech.*, vol. 38, pp. 1831–1836, Dec. 1990.

[17] M. Tsuji, S. Ueki, and H. Shigesawa, "Significant contribution of nonphysical leaky mode to the fields excited by a practical source in printed-circuit transmission lines," in *IEEE MTT-S Int. Microwave Symp. Dig.*, June 2002, pp. 957–960.

**William L. Langston** (S'95) was born in Houston, TX, on September 30, 1975. He received the B.S.E.E. (*magna cum laude*) and M.S.E.E. degrees from the University of Houston, Houston, TX, in 1999 and 2001, respectively, and is currently working toward the Ph.D. degree in electrical engineering at the University of Houston.

From 1999 to 2003, he was a Research Assistant with the Department of Electrical and Computer Engineering, University of Houston. His research interests include leakage effects in microwave integrated circuits, and microstrip antennas.

**Jeffery T. Williams** was born in Kula, Maui, Hawaii on July 24, 1959. He received the B.S., M.S., and Ph.D. degrees in electrical engineering from the University of Arizona, Tucson, in 1981, 1984, and 1987, respectively.

In 1987, he joined the Department of Electrical and Computer Engineering, University of Houston, Houston, TX, where he is currently a Professor. He was a Schlumberger-Doll Research Fellow with the University of Arizona. From 1983 to 1986, he spent four summers as a Research Scientist with the Schlumberger-Doll Research Center, Ridgefield, CT. From 1981 to 1982, he was a Design Engineer with the Zonge Engineering and Research Organization, Tucson, AZ, and as a Summer Engineer with the Lawrence Livermore National Laboratory, Livermore, CA. His research interests include the design and analysis of high-frequency antennas and circuits, high-frequency measurements, propagation on printed-circuit lines, and high-frequency materials. He was an Associate Editor for *Radio Science*.

Dr. Williams is a member of the International Scientific Radio Union (URSI) Commission B. He was an associate editor for the IEEE TRANSACTIONS ON ANTENNAS AND PROPAGATION.

**David R. Jackson** (S'83–M'84–SM'95–F'99) was born in St. Louis, MO, on March 28, 1957. He received the B.S.E.E. and M.S.E.E. degrees from the University of Missouri, Columbia, in 1979 and 1981, respectively, and the Ph.D. degree in electrical engineering from the University of California at Los Angeles (UCLA), in 1985.

From 1985 to 1991, he was an Assistant Professor with the Department of Electrical and Computer Engineering, University of Houston, Houston, TX. From 1991 to 1998 he was an Associate Professor with the same department and, since 1998, he has been a Professor. His current research interests include microstrip antennas and circuits, leaky-wave antennas, leakage and radiation effects in microwave integrated circuits, periodic structures, electromagnetic compatibility (EMC), and bioelectromagnetics. He is currently an Associate Editor for the *International Journal of RF and Microwave Computer-Aided Engineering*. He was an Associate Editor for *Radio Science*.

Dr. Jackson is currently the chapter activities coordinator for the IEEE Antennas and Propagation Society (IEEE AP-S) and the vice chair for URSI, U.S. Commission B. He is on the Editorial Board for the IEEE TRANSACTIONS ON MICROWAVE THEORY AND TECHNIQUES. He is a past distinguished lecturer for the IEEE AP-S. He is also a past associate editor for the IEEE TRANSACTIONS ON ANTENNAS AND PROPAGATION. He has also served as a member of the IEEE AP-S Administrative Committee (AdCom).

**Francisco Mesa** (M'94) was born in Cádiz, Spain, in April 1965. He received the Licenciado and Doctor degrees from the University of Seville, Seville, Spain, in 1989 and 1991, respectively, both in physics.

He is currently an Associate Professor in the Department of Applied Physics I, University of Seville. His research interest focuses on electromagnetic propagation/radiation in planar lines with general anisotropic materials.